Bioengineering Research

Studying the Physical Behavior of Human Mesenchymal Stem Cells on the Surface of Hydroxyapatite After Adding Graphene as A Reinforcement

Hassan Nosrati [1], Rasoul Sarraf-Mamoory *[1], Dang Quang Svend Le [2], Maria Canillas Perez [3], Cody Eric Bünger *[2]

[1]Department of Materials Engineering, Tarbiat Modares University, Tehran, Iran.
[2]Department of Clinical Medicine, Aarhus University, Denmark.
[3]Instituto de Cerámica y Vidrio, CSIC, Madrid, Spain.

Correspondence to: Sarraf-Mamoory R (E-mail: rsarrafm@modares.ac.ir)
Correspondence to: Bünger C (E-mail: codybung@rm.dk)

Abstract

Introduction: For cell culture assays, different cells have been used so far, including Mouse osteoblast cells (MC3T3-E1), hFOB cells, fibroblast cell, Osteoblast-like MG63 cells, Human osteoblast cells (HFOB 1.19 SV40 transfected osteoblasts), Blood mononuclear cell (PBMC), mesenchymal stem cells (MSCs).

Objective: In this study, the effect of graphene sheets on the physical behavior of stem cells was investigated.

Material and Methods: The hydrothermal method and spark plasma sintering were used in this study. The analysis performed in the sample includes X-ray diffraction, scanning electron microscope, Raman spectroscopy, and cell culture.

Result: The surface of the samples from the hydrophilic (in pure HA) state is somewhat close to the hydrophobic (in HA/rGO nanocomposites) state. It is clear that the physical behavior of the cells on the surface after graphene addition has changed dramatically.

Conclusion: The product of this research has the potential to be used in medical applications.

Keyword: Hydroxyapatite; Graphene; Stem Cell; Nanocomposites

Received: 24 December 2019, **Accepted**: 20 January 2020

DOI: 10.22034/jbr.2019.213164.1018

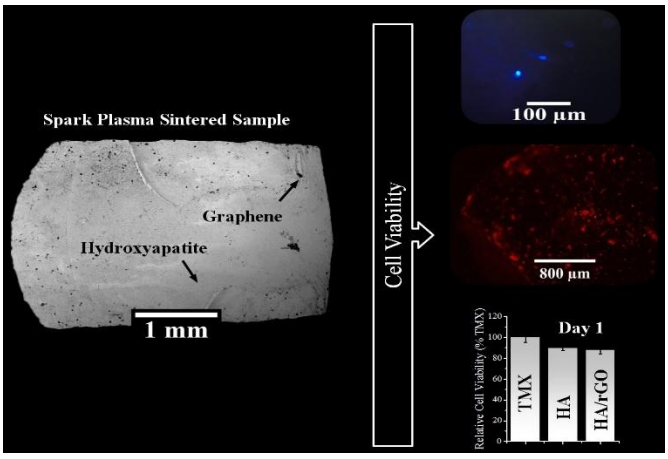

1. Introduction

Recently, hydroxyapatite (HA)/graphene nanocomposites have been much researched [1-5]. The main phases of these nanocomposites are HA and graphene. Additional components may be added for specific applications [6]. HA, with a chemical formula similar to that found in the mineral component of natural bone [7-9], has unique properties such as osteoconductivity, biocompatibility, and non-toxicity [10]. These properties have made HA widely used in the medical field, such as orthopedics [11]. But the mechanical properties of synthesized HA are very poor compared to natural bone and need to be improved by different strategies. One of these strategies is to use a reinforcement phase [12-14]. The reinforcement phase should be added in a limited amount to the main phase and not undermine the unique properties of HA. Among the materials used so far, carbon nanomaterials, especially graphene, have received much attention from researchers. The main reason for this is the excellent mechanical properties of graphene. The two-dimensional structure of graphene with high surface specific area has made it a good reinforcing property [15-17]. The biocompatibility and mechanical properties of graphene [18, 19] have not only improved the mechanical properties of HA, but also improved its biocompatibility properties.

There are various ways to synthesize these nanocomposites. Of all the available methods, chemical methods have become more popular because they are controllable and economical. Chemical methods for the synthesis of ceramics and composites include sol-gel [20-22], hydrothermal [23-25], and precipitation [26, 27]. Among these methods, the hydrothermal method due to the high pressure and temperature makes the powders with controlled morphology and high crystallinity without further heat treatment. Graphene oxide is used in this method because it contains surface agents that are suitable sites for the HA phase nucleation [28]. Published researches show that the presence of graphene as the reinforcing phase improves the mechanical and biologic properties of HA. For cell culture assays, different cells have been used so far, including mouse osteoblast cells (MC3T3-E1) [29, 30], hFOB cells [31], fibroblast cell [32], Osteoblast-like MG63 cells [33], human osteoblast cells (HFOB 1.19 SV40 transfected osteoblasts) [34], Blood mononuclear cell (PBMC) [35], mesenchymal stem cells (MSCs) [36, 37].

In previous reports, human mesenchymal stem cells and human fetal osteoblasts were used to investigate the biological properties of pure HA [38]. In this study, similar conditions were repeated for graphene-HA nanocomposites and the effect of graphene on the behavior of these cells were investigated. The hydrothermal method has been used to synthesize hybrid powders and the spark plasma sintering method has been used to consolidate them. The presence of graphene is expected to improve the biocompatibility properties. The results of this study will be useful for the applications of these composites as implants.

2. Materials and Methods

At the powder synthesis stage, the samples were synthesized according to a previously published report [39]. After powders characterization, the powders were consolidated by spark plasma sintering (SPS) method [38].

2.1. Powders characterization

The characterization methods used in this study with the specifications are listed in Table 1.

2.2. Cell culture

Human mesenchymal stem cells and human fetal osteoblasts were cultured on sintered samples exactly as in the previous paper [38], and the results were evaluated for one day, three days, and seven days. Figure 1 schematically illustrates the steps of this research.

3. Results and discussion

Figure 2 shows the results of the synthesized powders characterization. Figure. 2a shows Raman spectroscopy of the HA/rGO powders. The G peak determines the carbon-carbon stretching in the graphene, the peak D is related to structural defects, and the 2D peak is related to the number of layers of the graphene sheets. P-O symmetric stretching peaks at 962 cm^{-1} and 1049 cm^{-1} can be seen in the Raman

spectrum which confirms the formation of the HA phase. The results of this analysis confirm the presence of both phases in the synthesized powders [39-41].

The XRD patterns of powders (Figure. 2b) are in perfect agreement with the standard pattern of HA (JPCDS 09-0432). The XRD pattern of the HA/rGO powders is quite similar to pure HA. Graphene oxide (GO) has a peak in the range of 2θ=10. After reduction, the peak disappears and rGO peak appears from reduced GO that has a marked peak in the range of 2θ=26. Likely, the amorphous structure of rGO reduces its XRD peaks intensity compared to the pure HA. The peak in 2θ=26 for HA associated with the (002) plane is more intense than the peak for HA/rGO, and covers the graphene peak [39].

Figure. 2c shows the FTIR analysis of powders. After reduction of GO, the bonds associated with functional groups have been significantly reduced or disappeared (have been changed to higher absorption). These findings indicate that the synthesized powders contain rGO and HA [42, 43].

Table 1. The characterization methods used in this study

Analysis Method	Instrument Specification
XRD	X' Pert Pro, Panalytical Co.
FTIR	VERTEX 70, Brucker Co.
Raman spectroscopy	Reinshaw invia spectrometer
FESEM	Hitachi S4700

Figure 3 shows SEM images of the HA/rGO samples fracture surface after sintering process (SPS). The black spots on the Figure. 3a represent graphene sheets. Figure. 3b and 3c also show that the type of fracture in the composite differs from that of pure HA previously investigated [38]. This is due to the presence of graphene sheets in the composite structure.

Figure 4 shows fluorescent cell culture images on samples after 24 h and results of the MTT assay. Fig. 4a and 4b show the image (cell nucleus) of the cells stained for the HA/rGO composite sample. Figure. 4c-e show the cells skeleton. By comparing these images with those of the previous paper [38], it can be seen that the surface of the samples from the hydrophilic (in pure HA) state is somewhat close to the hydrophobic (in HA/rGO nanocomposites) state. The reason for this is that the graphene oxide is somewhat hydrophobic after reduction, leaving the effect on the surface. The results of MTT assay (Figure. 4f) shows the average value of the relative cell viability after 24 h, the significance level, and confidence interval of 95% (n = 8) obtained in the analysis of variance compared against the values obtained for TMX.

Figure 5 shows fluorescent cell culture images on samples after 72 h and results of the MTT assay. Figure. 5a shows the image (cell nucleus) of the cells stained for the HA/rGO composite sample after 72 h. Figure. 5b shows the cells skeleton. The results of MTT assay (Figure. 5c) shows the average value of the relative cell viability after 72 h, the significance level, and confidence interval of 95% (n = 8) obtained in the analysis of variance compared against the values obtained for TMX. After three days, the viability has decreased slightly but is still acceptable.

Figure 6 shows the results of MTT assay after seven days. The leachates obtained after 1 and 3 days had a significant effect on the survival of cells maintained in culture for 24 h. However, the decrease in relative cell viability with respect to negative control samples is not very significant, since in all cases these survival values are above 80% of the measurements for TMX. In contrast, the leachate obtained at 7 days did not significantly affect the viability of the osteoblasts used as the model, in which case cell viability was measured above 98%. It can be concluded that the leached obtained over a 7-day period showed no significant toxicity to the culture of the osteoblasts.

The presence of graphene has significantly improved the properties.

Figure 7 shows fluorescent cell culture images on composite samples after 168 h. Figure. 7d-f show the image (cell nucleus) of the cells stained for the HA/rGO composite sample. It is clear that the behavior of the cells on the surface after graphene addition has changed dramatically. The findings of this study, along with other published researches, will be useful in the development of tissue engineering [45-51].

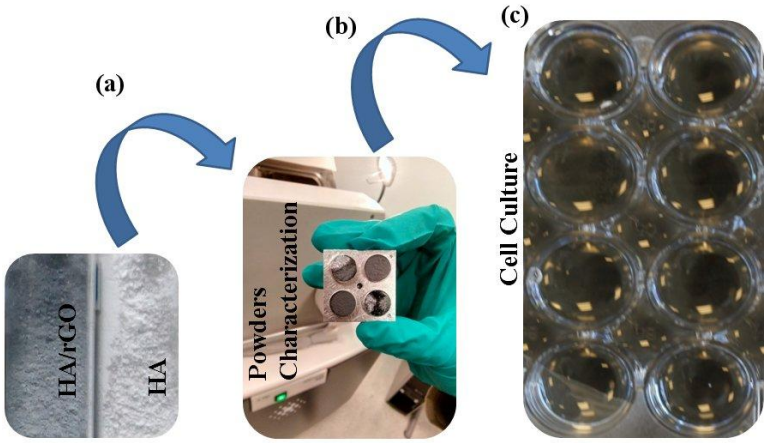

Figure 1. Research steps, a) HA and HA/rGO powders, b) characterization samples, c) cell culture

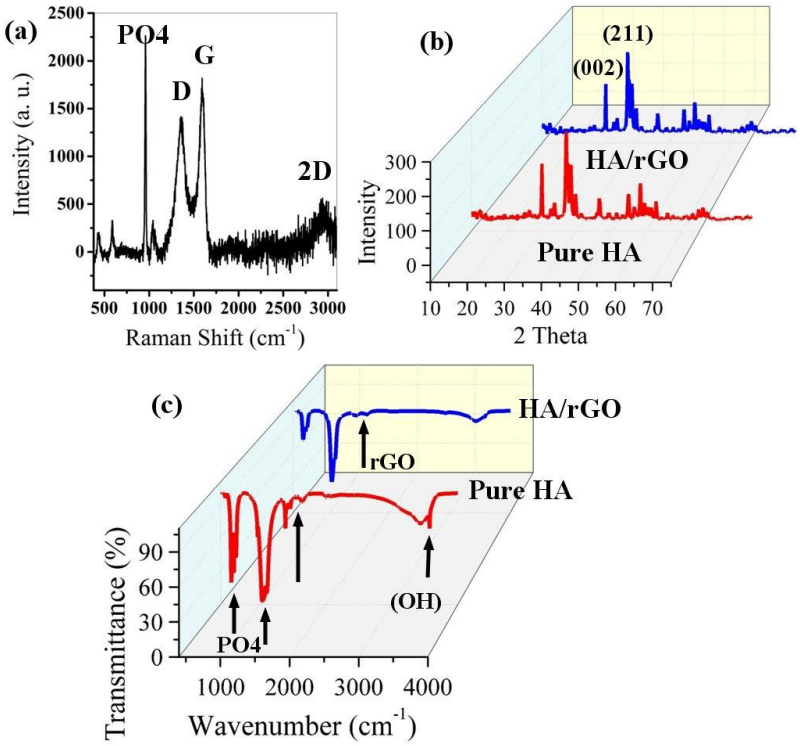

Figure 2. a) Raman spectroscopy of HA/rGO powders, b) XRD analysis of powders, c) FTIR analysis of powders

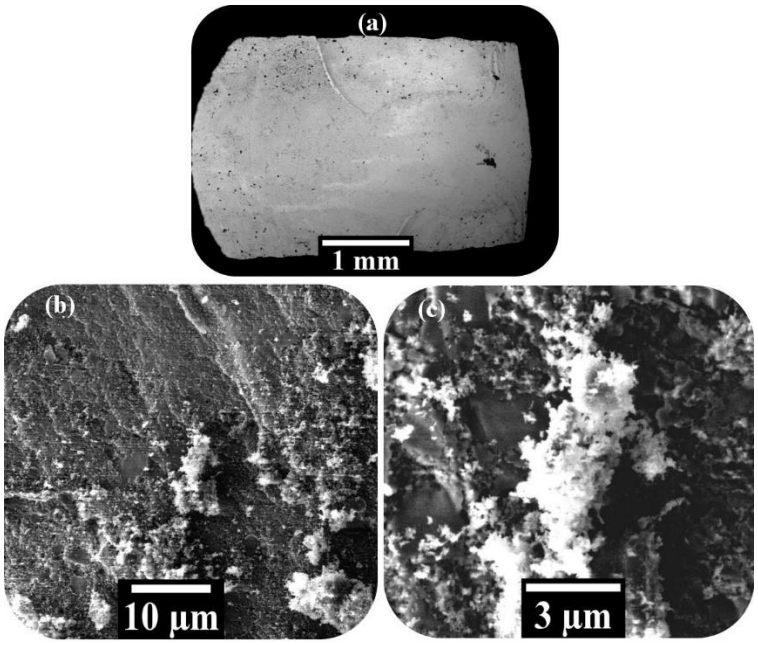

Figure 3: Fracture surface of the HA/rGO samples after sintering (SPS)

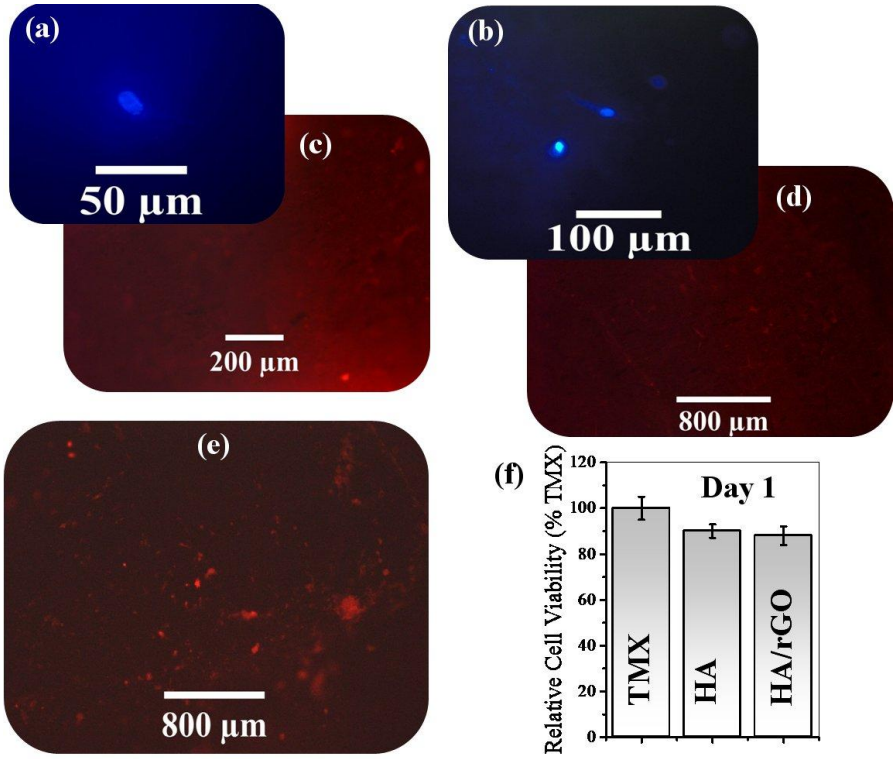

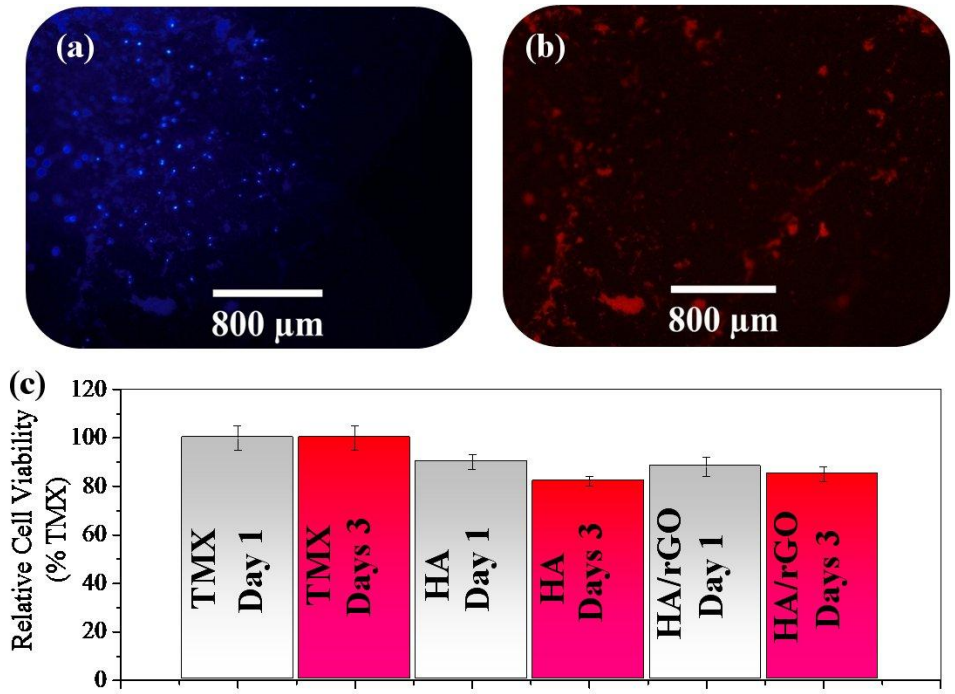

Figure 4: Fluorescent cell culture images on samples after 24 h and f) results of the MTT assay

Figure 5: Fluorescent cell culture images on samples after 72 h and c) results of the MTT assay

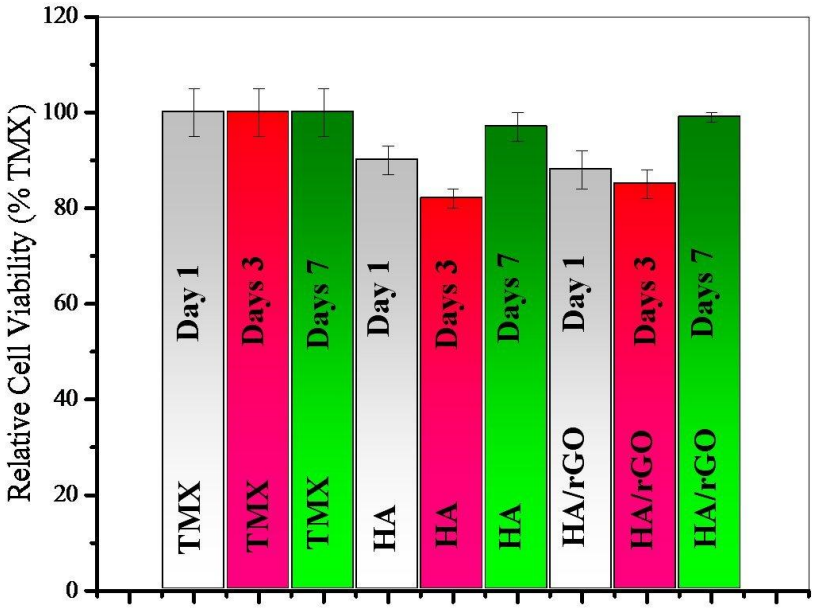

Figure 6: Results of the MTT assay after 168 h

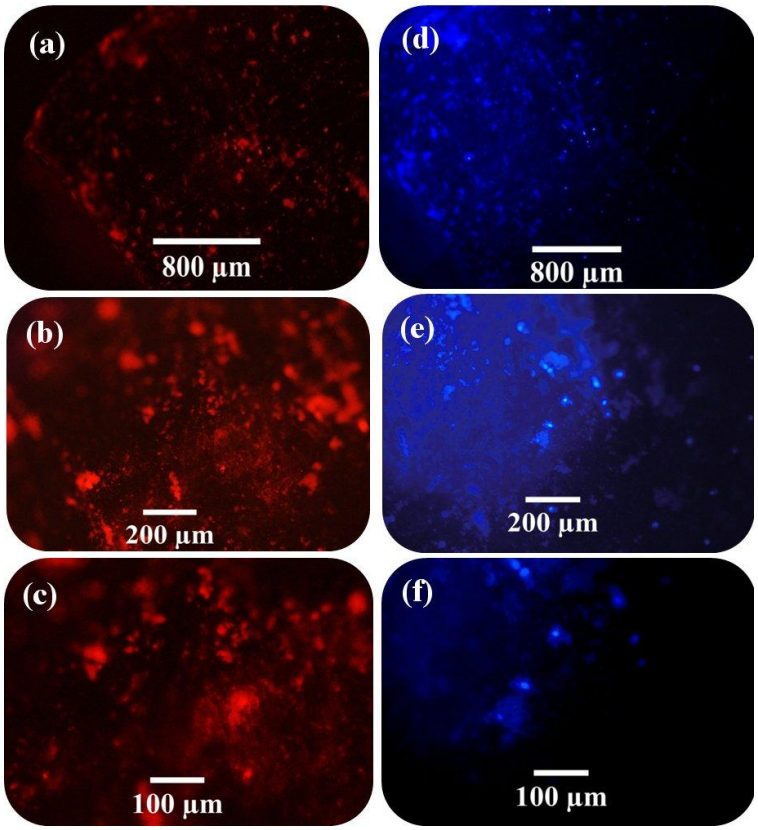

Figure 7: Fluorescent cell culture images on samples after 168 h

4. Conclusions

XRD, FTIR and Raman spectroscopy findings indicate that the synthesized powders contain rGO and HA. The type of fracture in the composite differs from that of pure HA. It can be seen that the surface of the samples from the hydrophilic (in pure HA) state is somewhat close to the hydrophobic (in HA/rGO nanocomposites) state. It is clear that the physical behavior of the cells on the surface after graphene addition has changed dramatically.

Conflict of interest

The authors certify that they have no affiliations with or involvement in any organization or entity with any financial interest, or non-financial interest in the subject matter or materials discussed in this manuscript.

Acknowledgments

No applicable.

References

[1] Q. Zhang, Y. Liu, Y. Zhang, H. Li, Y. Tan, L. Luo, J. Duan, K. Li and C. E. Banks, Facile and controllable synthesis of hydroxyapatite/graphene hybrid materials with enhanced sensing performance towards ammonia, Analyst 140 (2015) 5235–5242, DOI: 10.1039/c5an00622h

[2] C. Yao, J. Zhu, A. Xie, Y. Shen, H. Li, B. Zheng, Y. Wei, Graphene oxide and creatine phosphate disodium dual template-directed synthesis of GO/hydroxyapatite and its application in drug delivery, Materials Science and Engineering C 73 (2017) 709–715, http://dx.doi.org/10.1016/j.msec.2016.11.083

[3] C. Rodríguez-González, H. E. Cid-Luna, P. Salas,1 and V.M. Castaño, Hydroxyapatite-Functionalized Graphene: A New Hybrid Nanomaterial, Journal of

Nanomaterials (2014) 940903: 1-7, http://dx.doi.org/10.1155/2014/940903

[4] W. Xie, F. Song, R. Wang, S. Sun, M. Li, Z. Fan, B. Liu, Q. Zhang and J. Wang, Mechanically Robust 3D Graphene–Hydroxyapatite Hybrid Bioscaffolds with Enhanced Osteoconductive and Biocompatible Performance, Crystals 105 (8) (2018) 1-12, doi:10.3390/cryst8020105

[5] A. Rajesh, G. Mangamma, T.N. Sairam, S. Subramanian, S. Kalavathi, M. Kamruddin, S. Dash, Physicochemical properties of nanocomposite: Hydroxyapatite in reduced graphene oxide, Materials Science and Engineering C 76 (2017) 203–210, http://dx.doi.org/10.1016/j.msec.2017.02.044

[6] Q. Wang, Y. Chu, J. He, W. Shao, Y. Zhou, K. Qi, L. Wang, S. Cui, A graded graphene oxide-hydroxyapatite/silk fibroin biomimetic scaffold for bone tissue engineering, Materials Science and Engineering C 80 (2017) 232–242, http://dx.doi.org/10.1016/j.msec.2017.05.133

[7] M. Li, P. Xiong, F. Yan, S. Li, C. Ren, Z. Yin, A. Li, H. Li, X. Ji, Y. Zheng , Y. Cheng, An overview of graphene-based hydroxyapatite composites for orthopedic applications, Bioactive Materials 3 (2018) 1-18, https://doi.org/10.1016/j.bioactmat.2018.01.001

[8] V. Mišković-Stanković, S. Eraković, A. Janković, M. Vukašinović-Sekulić, M. Mitrić, Y. C. Jung, S. J. Park and K. Y. Rhee, Electrochemical synthesis of nanosized hydroxyapatite/ graphene composite powder, Carbon Letters 16 (4) (2015) 233-240, http://dx.doi.org/10.5714/CL.2015.16.4.233

[9] P. Yu, R-Y Bao, X-J Shi, W. Yang, M-B Yang, Self-assembled high-strength hydroxyapatite/grapheneoxide/chitosan composite hydrogel for bone tissue engineering, Carbohydrate Polymers 155 (2017) 507–515, http://dx.doi.org/10.1016/j.carbpol.2016.09.001

[10] X. Zhao, L. Zhang, X. Wang, J. Yang, F. He, Y. Wang, Preparation and mechanical properties of controllable orthogonal arrangement of carbon fiber reinforced hydroxyapatite composites, Ceramics International 44 (2018) 8322–8333, https://doi.org/10.1016/j.ceramint.2018.02.020

[11] X. Chen, B. Zhang, Y. Gong, P. Zhou, H. Li, Mechanical properties of nanodiamond-reinforced hydroxyapatite composite coatings deposited by suspension plasma spraying, Applied Surface Science 439 (2018) 60–65, https://doi.org/10.1016/j.apsusc.2018.01.014

[12] D-Y Kim, Y-H Han, J. H. Lee, I-K Kang, B-K Jang, and S. Kim, Characterization of Multiwalled Carbon Nanotube-Reinforced Hydroxyapatite Composites Consolidated by Spark Plasma Sintering, BioMed Research International (2014) 768254, 10 pages, http://dx.doi.org/10.1155/2014/768254

[13] S.P. Khanal, H. Mahfuz, A.J. Rondinone, Th. Leventouri, Improvement of the fracture toughness of hydroxyapatite (HAp) by incorporation of carboxyl functionalized single walled carbon nanotubes (CfSWCNTs) and nylon, Materials Science and Engineering C 60 (2016) 204–210, http://dx.doi.org/10.1016/j.msec.2015.11.030

[14] S. Kalmodia, S. Goenka, T. Laha, D. Lahiri, B. Basu, K. Balani, Microstructure, mechanical properties, and in vitro biocompatibility of spark plasma sintered hydroxyapatite–aluminum oxide–carbon nanotube composite, Materials Science and Engineering C 30 (2010) 1162–1169, doi:10.1016/j.msec.2010.06.009

[15] C. Gao, P. Feng, S. Peng, C. Shuai, Carbon nanotube, graphene and boron nitride nanotube reinforced bioactive ceramics for bone repair, Acta Biomaterialia 61 (2017) 1–20, http://dx.doi.org/10.1016/j.actbio.2017.05.020

[16] E. Gholibegloo, A. Karbasi, M. Pourhajibagher, N. Chiniforush, A. Ramazani, T. Akbari, A. Bahador, M. Khoobi, Carnosine-graphene oxide conjugates decorated with hydroxyapatite as promising nanocarrier for ICG loading with enhanced antibacterial effects in photodynamic therapy against Streptococcus mutans, Journal of Photochemistry & Photobiology, B: Biology 181 (2018) 14–22, https://doi.org/10.1016/j.jphotobiol.2018.02.004

[17] C. Fu, H. Bai, J. Zhu, Z. Niu, Y. Wang, J. Li, X. Yang, Y. Bai, Enhanced cell proliferation and osteogenic differentiation in electrospun PLGA/hydroxyapatite nanofibre scaffolds incorporated with graphene oxide, PLoS ONE 12(11) (2017) 0188352: 1-20, https://doi.org/10.1371/journal.pone.0188352

[18] J. J. Lee, Y. C. Shin, S-J Song, J. M. Cha, S. W. Hong, Y-J Lim, S. J. Jeong, D-W Han and B. Kim, Dicalcium Phosphate Coated with Graphene Synergistically Increases Osteogenic Differentiation In Vitro, Coatings 8 (13) (2018) 1-12, doi:10.3390/coatings8010013

[19] R. G. Bai, N. Ninan, K. Muthoosamy, S. Manickam, Graphene: A versatile platform for nanotheranostics and tissue engineering, Progress in Materials Science 91 (2018) 24–69, http://dx.doi.org/10.1016/j.pmatsci.2017.08.004

[20] H. Nosrati, N. Ehsani, H. Baharvandi, M. Mohtashami, H. Abdizadeh, V. Mazinani, Effect of primary materials

ratio and their stirring time on SiC nanoparticle production efficiency through sol-gel process, American Journal of Engineering Research (AJER) 3 (3) (2014) 317-321

[21] H. Nosrati, M. S. Hosseini, M. Nemati, A. Samariha, Production of TiO2 Nano-Rods Using Combination of Sol-Gel and Electrophoretic Methods, Asian Journal of Chemistry 25 (6) (2013) 3484-3486, http://dx.doi.org/10.14233/ajchem.2013.14250

[22] H. Nosrati, N. Ehsani, M. Nemati, A. Samariha, Changing pH to improve efficiency of SiC nano-particles produced by chemical method, Middle-East Journal of Scientific Research 12 (9) (2012) 1250-1253, DOI: 10.5829/idosi.mejsr.2012.12.9.366

[23] G. Bharath, Rajesh Madhu, Shen-Ming Chen, Vediyappan Veeramani, A. Balamurugan, D. Mangalaraj, C. Viswanathan and N. Ponpandian, Enzymatic electrochemical glucose biosensors by mesoporous 1D hydroxyapatite-on-2D reduced graphene oxide, J. Mater. Chem. B 3 (2015) 1360–1370, DOI: 10.1039/c4tb01651c

[24] M. Ramadas, G. Bharath, N. Ponpandian, A.M. Ballamurugan, Investigation on biophysical properties of Hydroxyapatite/Graphene oxide (HAp/GO) based binary nanocomposite for biomedical applications, Materials Chemistry and Physics 199 (2017) 179-184, http://dx.doi.org/10.1016/j.matchemphys.2017.07.001

[25] Z. Fan, J. Wang, Z. Wang, H. Ran, Y. Li, L. Niu, P. Gong, B. Liu, S. Yang, One-pot synthesis of graphene/hydroxyapatite nanorod composite for tissue engineering, CARBON 66 (2014) 407–416, http://dx.doi.org/10.1016/j.carbon.2013.09.016

[26] H. Nosrati, D. Q. S. Le, R. Z. Emameh, C. E. Bunger, Characterization of the precipitated Dicalcium Phosphate Dehydrate on the Graphene Oxide surface as a bone cement reinforcement, Journal of Tissues and Materials 2 (1) (2019) 33-46, DOI: 10.22034/jtm.2019.173565.1013

[27] A. H. Ahmadi, H. Nosrati, R. Sarraf-Mamoory, Decreasing β- three calcium phosphate particle size using graphite as nucleation sites and diethylene glycol as a chemical additive, Journal of Bioengineering Research 1(4) (2020), DOI:10.22034/JBR.2019.211371.1016

[28] K. L. S. Castro, R. V. Curti, J. R. Araujo, S. M. Landi, E. H. M. Ferreira, R. S. Neves, A. Kuznetsov, L. A. Sena, B. S. Archanjo, C. A. Achete, Calcium incorporation in graphene oxide particles: A morphological, chemical, electrical, and thermal study, Thin Solid Films 610 (2016) 10–18, http://dx.doi.org/10.1016/j.tsf.2016.04.042

[29] L. Zhang , W. Liu, C. Yue, T. Zhang , P. Li, Z. Xing , Y. Chen, A tough graphene nanosheet/hydroxyapatite composite with improved in vitro biocompatibility, CARBON 61 (2013) 105 –115, http://dx.doi.org/10.1016/j.carbon.2013.04.074

[30] J. H. Lee, Y. C. Shin, S-M Lee, O. S. Jin, S. H. Kang, S. W. Hong, C-M Jeong, J. B. Huh & D-W Han, Enhanced Osteogenesis by Reduced Graphene Oxide/Hydroxyapatite Nanocomposites, Scientific Reports 5 (2015) 18833: 1-13, DOI: 10.1038/srep18833

[31] R. Zhang, N. Metoki, O. Sharabani-Yosef, H. Zhu, and N. Eliaz, Hydroxyapatite / Mesoporous Graphene / Single-Walled Carbon Nanotubes Freestanding Flexible Hybrid Membranes for Regenerative Medicine, Adv. Funct. Mater. 26 (2016) 7965–7974, DOI: 10.1002/adfm.201602088

[32] L. Fathyunes, J. Khalil-Allafi, S. O. Reza Sheykholeslami, M. Moosavifar, Biocompatibility assessment of graphene oxide-hydroxyapatite coating applied on TiO2 nanotubes by ultrasound-assisted pulse electrodeposition, Materials Science & Engineering C 87 (2018) 10–21, https://doi.org/10.1016/j.msec.2018.02.012

[33] Y. Zeng, X. Pei, S. Yang, H. Qin, H. Cai, S. Hu, L. Sui, Q. Wan, J. Wang, Graphene oxide/hydroxyapatite composite coatings fabricated by electrochemical deposition, Surface & Coatings Technology 286 (2016) 72–79, http:// dx.doi.org/ 10.1016/ j.surfcoat. 2015.12.013

[34] Y. Liu, J. Huang, H. Li, Synthesis of hydroxyapatite–reduced graphite oxide nanocomposites for biomedical applications: oriented nucleation and epitaxial growth of hydroxyapatite, J. Mater. Chem. B 1 (2013) 1826–1834, DOI: 10.1039/c3tb00531c

[35] M. Đošic, S. Erakovic, A. Jankovic, M. Vukašinovic-Sekulic, I. Z. Matic, J. Stojanovic, K. Y. Rhee, V. Miškovic-Stankovic, S-J Park, In vitro investigation of electrophoretically deposited bioactive hydroxyapatite/chitosan coatings reinforced by graphene, Journal of Industrial and Engineering Chemistry 47 (2017) 336–347, http://dx.doi.org/10.1016/j.jiec.2016.12.004

[36] X. Xie, K. Hu, D. Fang, L. Shang, S. D. Tran and M. Cerruti, Graphene and hydroxyapatite self-assemble into homogeneous, free standing nanocomposite hydrogels for bone tissue engineering, Nanoscale 7 (2015) 7992–8002, DOI: 10.1039/c5nr01107h

[37] H. Fadol, S.G.A. Yafei, K. Uzun, F. Musharavati, E. Zalnezhad, A.M.S. Hamouda, C-O Yun, F. Jaber,

HA/rGO/Pd nanocomposite thin film coating on SST 304 - Synthesize, characterization, and properties

[38] investigations, Journal of Alloys and Compounds 741 (2018) 562-574, https://doi.org/ 10.1016/ j.jallcom. 2018.01.047

[39] H. Nosrati, R. Sarraf Mamoory, D. Q. S. Le, C. E. Bunger, R. Zolfaghari Emameh, F. Dabir, Gas injection approach for synthesis of hydroxyapatite nanorods via hydrothermal method, Materials Characterization 2019; 110071, https://doi.org/10.1016/j.matchar.2019.110071

[40] H. Nosrati, R. Sarraf-Mamoory, D. Q. S. Le, C. E. Bunger, Preparation of reduced graphene oxide/hydroxyapatite nanocomposite and evaluation of graphene sheets/hydroxyapatite interface, Diamond & Related Materials 100 (2019) 107561, https://doi.org/10.1016/j.diamond.2019.107561

[41] H. Nosrati, R. Sarraf Mamoory, F. Dabir, M. C. Perez, M. A. Rodriguez, D. Q. S. Le, C. E. Bünger, In situ synthesis of three dimensional graphene/hydroxyapatite nano powders via hydrothermal process, Materials Chemistry and Physics 222 (2019) 251–255, https://doi.org/10.1016/j.matchemphys.2018.10.023

[42] H. Nosrati, R. Sarraf Mamoory, F. Dabir, D. Q. S. Le, C. E. Bunger, M. C. Perez, M. A. Rodriguez, Effects of hydrothermal pressure on in situ synthesis of 3D graphene/hydroxyapatite nano structured powders, Ceramics International 45 (2019) 1761–1769, https://doi.org/10.1016/j.ceramint.2018.10.059

[43] H. Nosrati, R. Sarraf-Mamoory, D. Q. S. Le, C. E. Bunger, Fabrication of gelatin/hydroxyapatite/3D-graphene scaffolds by a hydrogel 3D-printing method, Materials Chemistry and Physics 239 (2020) 122305, https://doi.org/10.1016/j.matchemphys.2019.122305

[44] H. Nosrati, R. Sarraf-Mamoory, F. Dabir, Crystallographic study of hydrothermal synthesis of hydroxyapatite nano-rods using Brushite precursors, Journal of Tissues and Materials 2 (3) (2019) 1-8, DOI: 10.22034/jtm.2019.199830.1022

[45] H. Nosrati, R. Sarraf-Mamoory, D.Q.S. Le, C.E. Bünger, Enhanced fracture toughness of three dimensional graphene- hydroxyapatite nanocomposites by employing the Taguchi method, Composites Part B: Engineering 190 (2020) 107928; https://doi.org/10.1016/j.compositesb.2020.107928

[46] H. Nosrati, R. Sarraf-Mamoory, D.Q.S. Le, M.C. Perez, C.E. Bünger, Evaluation of Argon-Gas-Injected Solvothermal Synthesis of Hydroxyapatite Crystals Followed by High-Frequency Induction Heat Sintering, Cryst. Growth Des. 20(5) (2020) 3182-3189; https://doi.org/10.1021/acs.cgd.0c00048

[47] H. Nosrati, R. Sarraf-Mamoory, A.H. Ahmadi, M.C. Perez, Synthesis of Graphene Nanoribbons–Hydroxyapatite Nanocomposite Applicable in Biomedicine and Theranostics, J. Nanotheranostics 1(1) (2020) 2; https://doi.org/10.3390/jnt1010002

[48] A. Aidun, A.S. Firoozabady, M. Moharrami, A. Ahmadi, N. Haghighipour, S. Bonakdar, Graphene oxide incorporated polycaprolactone/chitosan/collagen electrospun scaffold: Enhanced osteogenic properties for bone tissue engineering, Artifical Organs 43(10) (2019) 264-281; https://doi.org/10.1111/aor.13474

[49] F. Ghorbani, A. Zamanian, A. Shams, A. Shamoosi, A. Aidun, Fabrication and characterisation of super-paramagnetic responsive PLGA–gelatine–magnetite scaffolds with the unidirectional porous structure: a physicochemical, mechanical, and in vitro evaluation, IET Nanobiotechnology 13(8) (2019) 860 – 867; https://doi.org/10.1049/iet-nbt.2018.5305

[50] H.Z. Marzouni, F. Tarkhan, A. Aidun, K. Shahzamani, H.R. Jahan Tigh, S. Malekshahian, H.E. Lashgarian, Cytotoxic Effects of Coated Gold Nanoparticles on PC12 Cancer Cell, Galen Medical Journal 7 (2018); http://dx.doi.org/10.22086/gmj.v0i0.1110

[51] A. Aidun, A. Zamanian, F. Ghorbani, Immobilization of polyvinyl alcohol-siloxane on the oxygen plasma-modified polyurethane-carbon nanotube composite matrix, Applied Polymer 137(12) (2020) 48477; https://doi.org/10.1002/app.48477.